

Variation in functional connectivity along anterior-to-posterior intraparietal sulcus, and relationship with age across late childhood and adolescence



Sarah A. Vinette ^{a,b,d}, Signe Bray ^{a,b,c,d,*}

^a Alberta Children's Hospital Research Institute, Room 293, Heritage Medical Research Building, 3330 Hospital Drive, NW, Calgary, AB, Canada T2N 4N1

^b Department of Radiology, Cumming School of Medicine, University of Calgary, Room 812, North Tower, Foothills Medical Centre, 1403 – 29th Street NW, Calgary, AB, Canada T2N 2T9

^c Department of Paediatrics, Cumming School of Medicine, University of Calgary, 2888 Shaganappi Trail NW, Calgary, AB, Canada T3B 6A8

^d Child and Adolescent Imaging Research Program, Alberta Children's Hospital, 2888 Shaganappi Trail NW, Calgary, AB, Canada T3B 6A8

ARTICLE INFO

Article history:

Received 29 September 2014

Received in revised form 12 April 2015

Accepted 13 April 2015

Available online 21 April 2015

Keywords:

Functional connectivity

Resting-state fMRI

IPS

Visual-spatial

Attention

Visuotopic

ABSTRACT

The intraparietal sulcus (IPS), a region in the dorsal attention network (DAN), has been implicated in multi-sensory attention and working memory. Working memory and attention develop across childhood; changes in functional connectivity within the DAN may relate to this maturation. Previous findings regarding fronto-parietal intrinsic functional connectivity age-effects were mixed. Our study aimed to circumvent limitations of previous work using a large cross-sectional sample, 183 typically developing participants 6.5–20 years, from the Autism Brain Imaging Data Exchange, and seed regions along the anterior-to-posterior axis of the IPS. These seeds, IPS0–4, were entered into functional connectivity models. Group-level models investigated differential connectivity along the IPS and relationships with age. Anterior IPS3/4 exhibited greater connectivity with sensorimotor/pre-motor regions. Posterior IPS0/1 demonstrated greater connectivity with dorsal and ventral visual regions. Positive age-effects were found between IPS3–4 and visual regions. Negative age-effects were found between IPS and superior parietal and medial orbitofrontal cortices. Follow-up region of interest analyses were used to estimate age-effects for DAN and anticorrelated default mode network regions. Results suggest age-effects on IPS functional connectivity are relatively modest, and may differ pre- and across-adolescence. Studying typical age-related connectivity variability within this network may help to understand neurodevelopmental disorders marked by impaired attention.

© 2015 The Authors. Published by Elsevier Ltd. This is an open access article under the CC BY-NC-ND license (<http://creativecommons.org/licenses/by-nc-nd/4.0/>).

Abbreviations: IPS, intraparietal sulcus; hFEF, putative human frontal eye fields; hSMA, human supplementary motor area; DLPFC, dorsolateral prefrontal cortex; MT, middle temporal; fMRI, functional magnetic resonance imaging; TD, typically developing; ABIDE, Autism Brain Imaging Data Exchange; IRB, institutional review board; FWHM, full width at half maximum; WM, white matter; CSF, cerebrospinal fluid; FWE, family wise error; DAN, dorsal attention network; FPN, fronto-parietal network; DMN, default mode network; ROI, region-of-interest; TPJ, temporoparietal junction; ASD, autism spectrum disorders; TR, repetition time; TE, echo time; FOV, field of view; MNI, Montreal Neurological Institute; VLPFC, ventrolateral prefrontal cortex; SM, sensorimotor; FG, fusiform gyrus; Calc, peri-calcarine cortex; OT, occipito-temporal; MO, mid occipital; PT, posterior thalamus; VMPFC, ventromedial prefrontal cortex; IPL, inferior parietal lobule; PCUN, precuneus; Mid Temp, middle temporal; CN, caudate nucleus; WASI, Wechsler Abbreviated Scale of Intelligence; DAS, Differential Ability Scales; PPVT, Peabody Picture Vocabulary Test; FIQ, Full Scale IQ; VIQ, Verbal IQ; PIQ, Performance IQ; BA, Brodmann area; BOLD, blood oxygenation level-dependent.

* Corresponding author at: 2888 Shaganappi Trail NW, Calgary, AB, Canada T3B 6A8. Tel.: +1 403 955 7389.

E-mail addresses: savinett@ucalgary.ca (S.A. Vinette), sibray@ucalgary.ca (S. Bray).

1. Introduction

The intraparietal sulcus (IPS) is located along the dorsal visual pathway and is a key node in the network underlying spatial attention (Astafiev et al., 2003; Corbetta et al., 2000; Goodale and Milner, 1992; Silver and Kastner, 2009). This functionally heterogeneous brain region has also been implicated in multisensory attention (Anderson et al., 2010), working memory (Champod and Petrides, 2007; Pessoa et al., 2002), and numerical cognition (Cantlon and Li, 2013; Dehaene et al., 2003; Pinel et al., 2001; Rosenberg-Lee et al., 2011). The IPS is a core node of the dorsal attention (Power et al., 2011) or task-positive network (Fox et al., 2005; Toro et al., 2008), which includes putative human frontal eye fields (hFEF) and supplementary motor area (hSMA) as well as dorsolateral prefrontal cortex (DLPFC) and occipito-temporal regions (near human middle temporal (MT)+).

The IPS can be divided into a set of regions spanning the anterior-to-posterior axis, on the basis of phase reversals in topographic organization, similar to retinotopic visual cortex (Sereno et al., 2001). These regions show differences in functional responses across tasks (Bray et al., 2013a; Sheremata et al., 2010; Silver and Kastner, 2009; Swisher et al., 2007; Szczepanski et al., 2013), and differential white matter structural connectivity to visual regions and parts of the dorsal attention network (Bray et al., 2013b; Greenberg et al., 2012; Szczepanski et al., 2013). In these studies, structural connectivity is defined using probabilistic tractography to determine the likelihood that two regions are joined by a direct white matter pathway. With regards to the IPS, posterior regions show preferential connectivity with dorsal and ventral visual regions (Bray et al., 2013b; Greenberg et al., 2012), while anterior regions show more probable connections to prefrontal and pre-motor regions (Bray et al., 2013b; Mars et al., 2011; Szczepanski et al., 2013). Lesion studies (Vandenbergh et al., 2012) and task activation and connectivity studies (Hutchinson et al., 2015) further support functional sub-divisions along the IPS.

Visual-spatial attention and working memory mature across late childhood and adolescence (Westerberg et al., 2004; Zhan et al., 2011). Functional connectivity is a measure believed to reflect the synchrony between brain regions (Friston, 1994), and is often calculated as the temporal correlation between pairs of time-series. Changes in functional and structural/white matter connectivity with age are hypothesized to be a key driver of cognitive maturation (Blakemore, 2012; Fair et al., 2007; Rubia, 2013; Supekar et al., 2009; Uddin et al., 2011). In support of this view, protracted development of white matter structure has been observed through early adulthood (Lebel et al., 2008). Age-related variation in fronto-parietal white matter properties across childhood has been linked to increased working memory capacity (Nagy et al., 2004; Østby et al., 2011), and visual-spatial attention (Klarborg et al., 2013).

Findings regarding age-effects on fronto-parietal functional connectivity have been mixed. Several developmental neuroimaging studies have shown increased functional magnetic resonance imaging (fMRI) blood oxygenation level-dependent (BOLD) signal during working memory tasks, relative to baseline, in frontal and parietal regions with age-related increases in working memory capacity (Crone et al., 2006; Klingberg et al., 2002; Scherf et al., 2006). Computational modeling has further suggested that fronto-parietal connectivity underlies inter-individual differences in working memory capacity (Edin et al., 2007). In resting-state connectivity studies, although somewhat controversial due to inconsistencies in handling motion artifacts (Power et al., 2012), a general pattern of increasing long-range connectivity with age has been described (Dosenbach et al., 2010; Fair et al., 2007). The spatial pattern of attention networks in children 5–8 years of age has been reported to be fragmented and incomplete compared to the same networks seen in adults (de Bie et al., 2012). In older children,

while differences compared to adults in IPS-to-DPLFC connectivity have been observed (Barber et al., 2013), other work has found no difference in fronto-parietal functional connectivity (Jolles et al., 2011; Uddin et al., 2011).

Several factors may contribute to variability in findings regarding developmental changes, or age-related variability, in fronto-parietal functional connectivity, including differential sensitivity of task compared resting scans, analysis approach, and small sample size. Among studies that have used region-of-interest (ROI) approaches, choice of seed region may also impact findings, as there is considerable heterogeneity of function and connectivity within both prefrontal (Kahnt et al., 2012; Liu et al., 2013; Moayedi et al., 2014) and parietal (Anderson et al., 2011; Mars et al., 2011; Nelson et al., 2010) cortices.

Developmental abnormalities in the IPS have been linked with aberrant numerical and visuospatial cognition (Auzias et al., 2014; Bray et al., 2011; Kesler et al., 2004, 2006; Molko et al., 2003; Nordahl et al., 2007). Therefore, characterizing age-related variability in fronto-parietal functional connectivity is important, both for understanding the neural basis of typical cognitive maturation, and as a baseline for comparing atypical development. The present study investigated age-related variability in IPS functional connectivity across childhood and adolescence, and aimed to circumvent limitations of previous work by (1) using a large database of resting-state fMRI data, and (2) using multiple seeds along the anterior-to-posterior axis of the IPS, in locations corresponding to previously defined IPS0-4 (Swisher et al., 2007) with well characterized patterns of structural connectivity (Bray et al., 2013b; Greenberg et al., 2012; Szczepanski et al., 2013).

We hypothesized that IPS sub-regions would show varying functional connectivity with visual and prefrontal regions along the anterior-to-posterior axis, consistent with previous work (Mars et al., 2011). Specifically, we hypothesized that anterior regions of the IPS would be more strongly functionally connected with frontal regions of the network including hFEF, whereas posterior IPS regions would have greater functional connectivity with visual regions. We further hypothesized differential age-related variability in functional connectivity. Specifically, we hypothesized that as primary sensory brain systems have been shown to mature relatively early (Gogtay et al., 2004; Shaw et al., 2008; de Bie et al., 2010), posterior IPS-to-occipital connectivity patterns would be relatively stable, while anterior IPS-to-prefrontal (e.g. DLPFC Barber et al., 2013) connectivity would show a positive association with age.

2. Materials and methods

2.1. Participants

Typically developing (TD) participants less than 20 years of age were included the analyses from four sites from the Autism Brain Imaging Data Exchange (ABIDE; http://fcon_1000.projects.nitrc.org/indi/abide/) database (Di Martino et al., 2014). These four sites included the New York University Langone Medical Centre, University of Michigan (samples one and two), University of Utah School of Medicine, and the Yale Child Study Centre. These sites were chosen as they had more than 20 TD participants younger than 20 years of age, with an age span greater than 10 years across participants. The research protocols were approved by the institutional review board (IRB) at each site. While inclusion and exclusion criteria differed across the sites, TD participants were generally excluded if they had a history of neurodevelopmental or psychiatric diagnosis, neurological disorder or any contraindications for MRI (Supplementary Table 1). Written consent and assent were obtained as appropriate from all participants at each of the sites.

Table 1

Participant characteristics by ABIDE database site.

Site	# Participants	Max age (years)	Min age (years)	Age range (years)	Mean age ± standard deviation (years)	Gender F	Handedness		Eyes Op
							Lt	Un	
New York University Langone Medical Centre	77	19.73	6.47	13.26	12.71 ± 3.27	19	2	3	13
University of Michigan: Samples one and two	64	19.2	8.20	11.00	14.72 ± 2.85	16	8	3	0
University of Utah School of Medicine	19	19.76	9.95	9.80	16.08 ± 2.80	0	2	0	0
Yale Child Study Center	23	17.83	7.66	10.17	12.80 ± 2.78	6	4	0	0
Total	183	19.76	6.47	13.29	13.78 ± 3.23	41	16	6	13

F=females; Lt=left; Un=unknown; Op=opened.

In total, 203 participants met the criteria to be included in this study. Participants were excluded from analyses for various reasons including: 25% or more of the volumes significantly impacted by motion (15), poor data quality (2), and difficulties with data processing (3). As a result, 183 participants (142 male, 41 female, age range: 6.47–19.76 years) were included in the final analysis (**Table 1**). For sites where a quantitative measure was reported for participants' handedness, positive values were identified as right-handed and negative values were identified as left-handed, resulting in a binary measure of handedness. In 6 cases, handedness was not reported; for the purposes of analyses, these participants were categorized as right-handed. Information regarding participants' Full Scale IQ (FIQ) scores can be found in Supplementary Table 2; for participants included in this analysis, FIQ scores ranged from 73 to 144.

2.2. Neuroimaging data

Neuroimaging data at each site was acquired using a 3T MR scanner and included T2*-weighted BOLD scans 6–10 min in length as well as T1-weighted anatomical scans. Functional and anatomical image acquisition parameters and procedure varied by site with image resolution varying from 3 to 4 mm³ and 1 to 1.4 mm³ for functional (**Table 2**) and anatomical volumes respectively. Whole-brain T1-weighted images were used in the pre-processing of functional images for all sites however were not analyzed.

2.3. Pre-processing

Standard pre-processing steps for fMRI analyses were conducted using SPM (<http://www.fil.ion.ucl.ac.uk/spm/software/>)

spm8/) software in MATLAB (Mathworks, Natick, MA). Pre-processing included: slice timing correction, realignment to the third volume acquired, spatial smoothing using a 4 mm FWHM Gaussian kernel, and artifact detection and repair of volumes with more than 0.5 mm/TR of motion using the ArtRepair toolbox (Mazaika et al., 2009). Functional images were then coregistered to the T1-weighted images. Automatic anatomical segmentation was performed and a 95% probability threshold was applied to the white matter (WM) and cerebrospinal fluid (CSF) masks. These thresholded masks were used to extract mean WM and CSF time courses from functional scans. The WM and CSF time courses were included in a regression analysis along with the motion parameters using in-house scripts. The residual data were band pass filtered using a low pass and high pass cutoff of 0.1 and 0.001 Hz respectively. Finally, to assist with standardizing data across sites, all brain voxels were set to a mean of 1000 and time courses were converted to Z-scores. The functional data were then normalized to the MNI template, resampled to 2 mm³, and spatially smoothed using a 7 mm FWHM Gaussian kernel.

2.4. IPS region-of-interest (ROI) definition

Left and right IPS0-4 ROIs were created using the MarsBaR MATLAB toolbox (Brett et al., 2002). Spherical ROIs with a radius of 3 mm, shown in **Fig. 1**, were created using the locations of IPS0-4 identified in Swisher et al. (2007). These coordinates were shifted by a maximum of 1.73 mm in order to generate ROIs of equal size (19 voxels) (**Table 3**). Such an alteration in the location of each ROI is well within the variance observed across participants (Swisher et al., 2007).

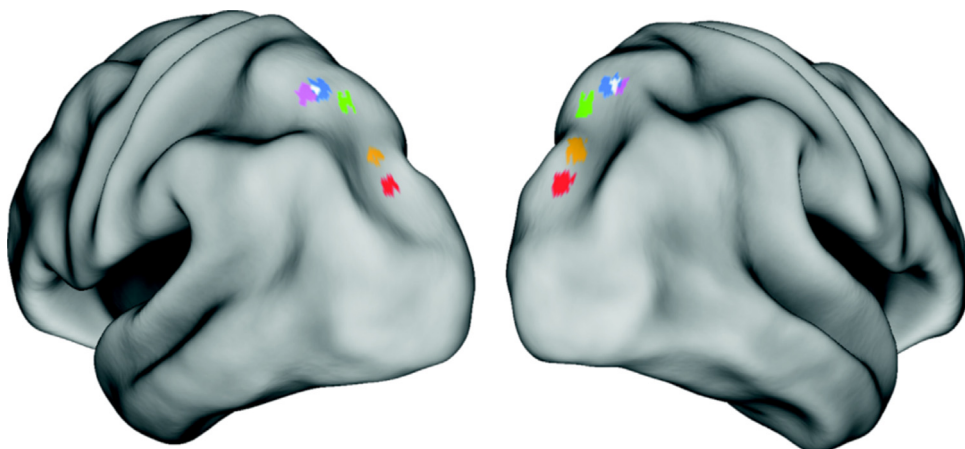


Fig. 1. Location of the left and right IPS seeds. Locations adapted from Swisher et al. (2007) (coordinates in **Table 3**) used in the seed-based functional connectivity analyses, overlaid on left and right hemisphere cortical surfaces. Purple = IPS4, Blue = IPS3, Green = IPS2, Orange = IPS1, Red = IPS0, White = the two-voxel overlap between IPS3 and IPS4.

Table 2
Functional imaging parameters and procedure for each ABIDE data collection site.

Site	Parameters						Procedure
	MR scanner	TR (s)	TE (ms)	# Slices	Slice thickness (mm)	Voxel size (mm ³)	
New York University Langone Medical Centre	3 T Siemens Allegro	2	15	33	4	3 × 3 × 4	90°
University of Michigan: Samples one and two	3 T GE Signa	2	30	40	3	3.4 × 3.4 × 3	90°
University of Utah School of Medicine Yale Child Study Center	3 T Siemens Trio	2	28	40	3	3.4 × 3.4 × 3	90°
	3 T Siemens Trio	2	25	34	4	3.4 × 3.4 × 4	60°

TR = repetition time; TE = echo time; FOV = field of view.

Table 3

Location of the IPS seed regions. Original locations from Swisher et al. (2007) were shifted slightly to obtain five regions of equal size (19 voxels).

Seed regions	MNI coordinates		
	x	y	z
IPS0	±26	-80	32
IPS1	±24	-74	40
IPS2	±22	-68	52
IPS3	±26	-62	56
IPS4	±26	-58	54

2.5. First-level functional connectivity models

Time courses were extracted by averaging signals over voxels included in each of the 10 IPS seeds, prior to the final spatial smoothing step. Multiple regression models were run for each participant with each of the 10 IPS seed regions as regressors (i.e., 10 models per participant). Volumes flagged as motion-corrupted by ArtRepair software were de-weighted prior to model estimation. Within this sample, there was no significant relationship between participant's age and the percentage of fMRI volumes corrupted due to motion ($p = 0.132$).

2.6. Group-level functional connectivity models

Group-level models were run for each seed separately in the left and right hemisphere, including an intercept term as well as effects of age and covariates of no interest: handedness, site of data collection, whether the participants had their eyes open or closed during the resting scan, and gender. Contrasts estimated the average connectivity pattern for each seed and the positive and negative associations with age. Models were also run that included all 5 seeds in each hemisphere in order to directly compare the connectivity patterns between seeds. Two contrasts were run, an F-contrast to identify any target locations with varying connectivity depending on the seed, and a T-contrast to identify a linear change in connectivity from posterior to anterior. As age-effects on connectivity may be more pronounced in younger or older participants across this age-range, a second set of models were run on median split data (median = 14). The younger (6–14 years) and older (14–20 years) subgroups included 90 and 93 participants, respectively.

2.7. Target ROI definition and IPS connectivity with target ROIs

As the hypothesized age-effects were not apparent at a whole-brain corrected statistical threshold, follow-up analyses were conducted in a priori ROIs to characterize the size of age-effects in this sample. Target ROIs were selected from a group-level model that included all 10 seeds, using positive and negative contrasts each averaging over all 10 seeds. Peak regions were chosen from these two contrasts (positive and negative) at a threshold of $p < 0.05$ family wise error (FWE) corrected. From the positive contrast, these generally corresponded to regions of the dorsal attention (DAN) or fronto-parietal network (FPN; Fox et al., 2005; Power et al., 2011); from the negative contrast, these were mainly regions that are part of the default mode network (DMN). For each pair of ipsilateral seeds and targets, a separate linear mixed model was run to estimate the effect of age on connectivity, with site as a grouping variable; additional covariates of no-interest included gender, handedness and eye status (open or closed). Models were run on the whole group ($N = 183$), as well as older and younger sub-groups ($N = 90, 93$ respectively).

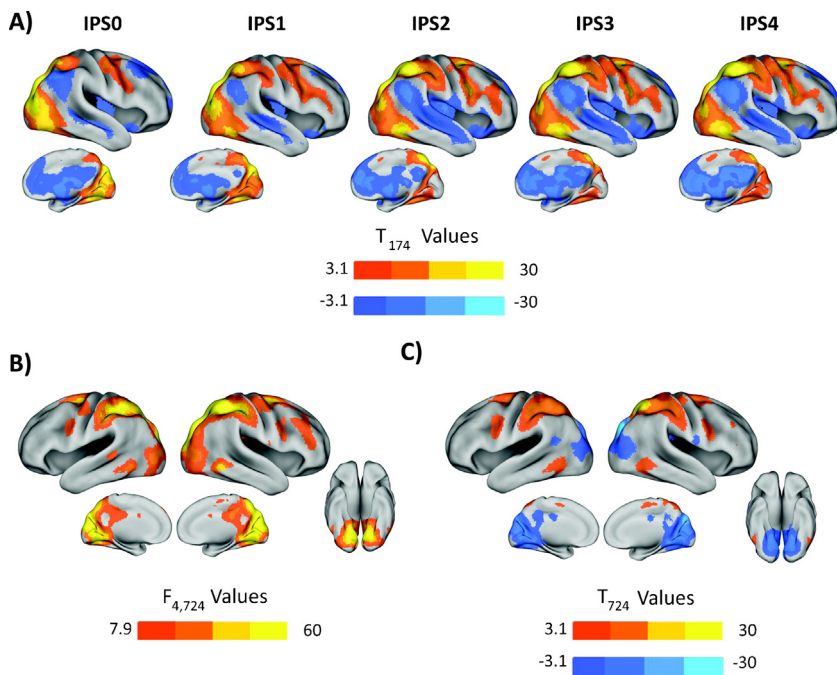


Fig. 2. Functional connectivity with, and differences across, right IPS seeds. (A) Positive and negative functional connectivity patterns for right IPS seeds 0–4. Warm colors indicate positive connectivity, while cool colors indicate negative. (B) Results of an F-contrast testing the main effect of seed on connectivity, for the five right hemisphere seeds. (C) A linear T-contrast testing anterior-to-posterior differences in functional connectivity. Warm colors indicate positive connectivity, while cool colors indicate negative. T-maps are thresholded at $p < 0.001$ and only clusters at $p < 0.05$ whole brain peak FWE corrected. F-maps are thresholded at $p < 0.05$ whole brain peak FWE-corrected.

3. Results

3.1. Functional connectivity for IPS0–4

Functional connectivity patterns for IPS0–4 are shown for the right hemisphere in Fig. 2A. Patterns were largely bilateral and effects were similar for the left hemisphere. Consistent with previous adult and child studies, we observed positive functional connectivity between IPS seeds and regions of the fronto-parietal or dorsal attention network including putative human FEF, occipito-temporal cortex (near MT) and dorsolateral prefrontal cortex (Barber et al., 2013; Farrant and Uddin, 2015; Fox et al., 2005). Also as expected, we observed negative connectivity with regions of the DMN including inferior parietal lobule, posterior cingulate/precuneus and medial prefrontal cortex (Fox et al., 2005; Greicius et al., 2009).

Although there are broad similarities in connectivity patterns across seeds, Fig. 2A suggests that there are differences in connectivity strength to both occipital and prefrontal regions. This was tested in Fig. 2B, which shows the results of an F-contrast, assessing the effect of seed. This confirms that there are differences in the strength of connectivity depending on the anterior-posterior location of the seed in occipital, fusiform, dorsal prefrontal and precuneus regions. Fig. 2C shows the results of a linear contrast for differences in connectivity along the anterior-to-posterior axis of the IPS, which shows that anterior parietal and dorsal prefrontal and premotor regions show stronger functional connectivity with anterior IPS, while occipital and fusiform regions show stronger connectivity with posterior seeds.

3.2. Age-effects

Significant positive and negative linear effects of age for IPS seeds are shown in Fig. 3. In the left hemisphere (left panels), IPS0 showed a positive age-association in right temporoparietal

junction (TPJ) ($[42 -36 12], n = 573, Z = 4.7$), IPS2 a negative association in bilateral superior parietal cortex ($[22 -48 52], n = 356, Z = 4.2; [-24 -44 50], n = 458, Z = 4.1$), and IPS3 showed a positive age-association with right fusiform ($[34 -40 -22], n = 373, Z = 4.0$) and negative with left superior parietal cortex ($[-24 -44 46], n = 376, Z = 4.2$).

In the right hemisphere (right panels), IPS1 showed a negative age-association with medial orbitofrontal cortex ($[0 60 -4], n = 327, Z = 4.2$), IPS3 showed a negative association with right superior parietal ($[20 -48 50], n = 411, Z = 4.8$) and IPS4 showed a positive association with bilateral fusiform ($[-24 -72 -4], n = 883, Z = 4.3; [22 -70 -6], n = 341, Z = 4.0$) and negative association with left parietal ($[-26 -38 38], n = 432, Z = 4.9$).

A second analysis was performed using functional runs that were truncated to be the same length across all sites (180 volumes). A third analysis was conducted including the percent of volumes de-weighted due to excessive motion as a covariate in the models. Results with these additional models were essentially the same and are listed in Supplementary Table 3.

We note that with the exception of the IPS0-TPJ pattern, age-effects occurred within regions that were positively or negatively connected to the IPS seed networks, on average. The negative parietal effects were anterior to IPS4 in regions positively connected to the seeds, on average. The positive fusiform effects were in regions that, though more strongly connected to IPS0, were still part of the average network for IPS3,4. The right IPS1 seed was on average negatively connected to the medial orbitofrontal region that showed a negative age-effect.

To allow for the possibility of age-effects that differ between adolescents and younger children, follow-up analyses were run in younger (6–14 years, $N = 90$) and older (14–20 years, $N = 93$) subsamples. In these models, only the right IPS2 showed a significant positive age-effect in left fusiform ($[-16 -50 -4], n = 290, Z = 3.8$) in the younger group. No other significant effects were found in either the younger or older sub-sample.

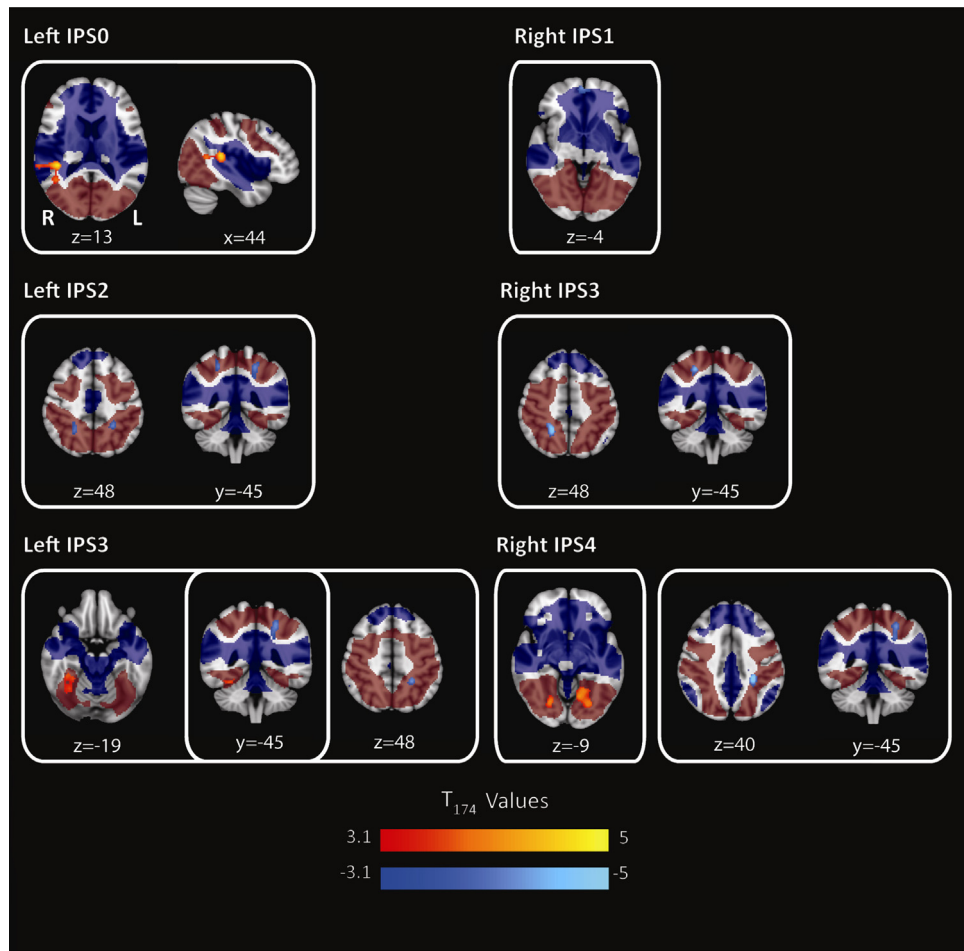


Fig. 3. Linear effects of age for each IPS seed region. Left panels: left hemisphere seeds, right panels: right hemisphere seeds. Positive effects in warm colors and negative effects in cool colors. T-maps are thresholded at $p < 0.001$ and only clusters at $p < 0.05$ FWE corrected are shown. The functional connectivity maps for each IPS seed are included in this figure as a dark red (positive network) and dark blue (negative network) transparent underlay. This underlay was thresholded at $p < 0.001$ with only clusters at $p < 0.05$ FWE corrected displayed.

3.3. Target ROI definition

From contrasts averaging positive and negative effects for all 10 IPS seeds (Fig. 4A), two sets of target ROIs were defined (Table 4). From the positive contrast, these generally correspond to regions of the dorsal attention (DAN) or fronto-parietal network (FPN; Fox et al., 2005; Power et al., 2011), such as the DLPFC and hFEF, but also included ventral visual (fusiform gyrus) and thalamic regions. From the negative contrast, these were mainly regions that are part of the default mode network (DMN).

3.4. Age-effects on connectivity to target ROIs

Parameter estimates for the age regressor from the linear mixed models with positive targets are shown in Fig. 5 ($*p < 0.05$, $**p < 0.005$), for the whole group, younger and older sub-groups. Over the entire sample, the only regions showing an age-regression slope with a p -value < 0.05 were left and right fusiform, left occipito-temporal and right peri-calcarine targets. These regions all showed increased connectivity with age to anterior IPS regions 3 and/or 4, and left VLPFC, which showed decreasing connectivity with IPS4 with increasing age. Age-effects were generally more positive in the younger group, with several prefrontal age-slopes significant at $p < 0.05$. In the oldest group, only left VLPFC showed a negative slope that reached $p < 0.05$.

Parameter estimates for linear age-effects with negative targets are shown in Fig. 6 ($*p < 0.05$, $**p < 0.005$). In the whole group, right inferior parietal showed a positive linear effect of age at $p < 0.05$, with right IPS4, and right middle frontal showed a significant negative age-effect with right IPS1. In contrast to the positive targets, which showed generally more positive effects in the younger age group, for negative targets the older age group showed more negative age-effects.

Age-effects in Figs. 5 and 6 were relatively modest and do not survive correction over all of the models estimated. However, visualization of parameter estimates can help to identify trends in the data and can be informative for planning future studies.

4. Discussion

This study investigated age-related variability, across late childhood and adolescence, in functional connectivity from a set of seeds along the posterior-to-anterior axis of the IPS. Though all IPS seeds showed robust functional connectivity with regions of the dorsal attention network, relative to one another, IPS0-4 have unique functional connectivity patterns: posterior IPS shows enhanced connectivity with dorsal and ventral visual regions, while anterior IPS shows greater connectivity with prefrontal and sensorimotor regions. Although we hypothesized a positive association with age specifically between anterior IPS and prefrontal regions, at a

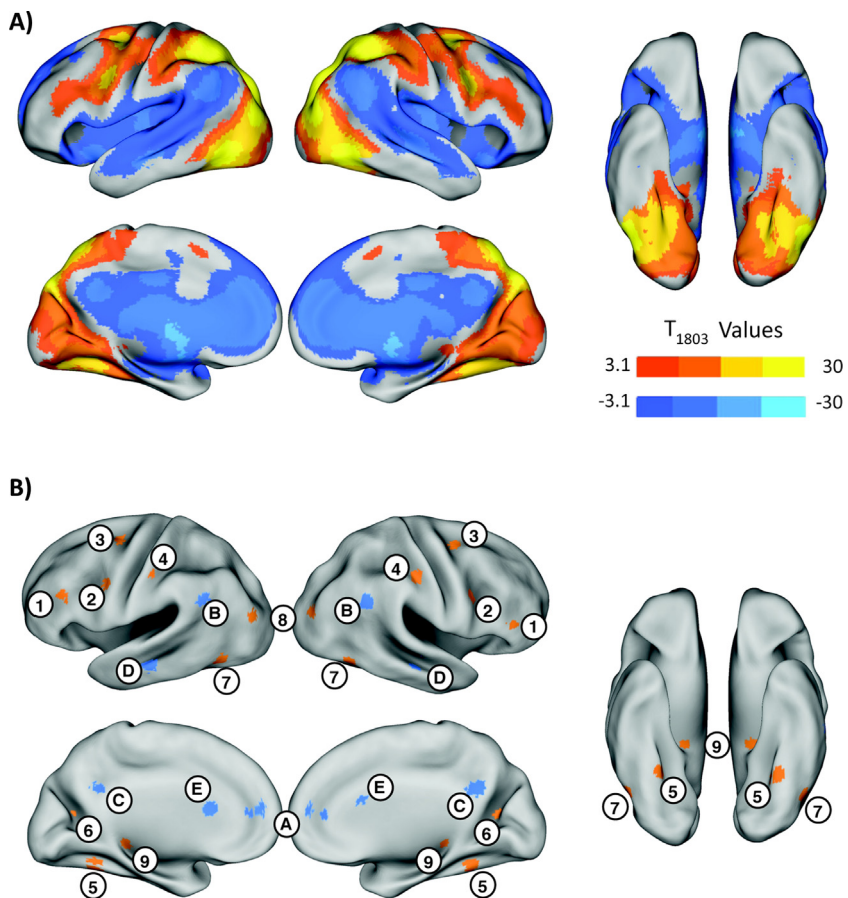


Fig. 4. IPS functional network. (A) Average network of brain regions functionally connected to bilateral IPS0-4 seeds with warm colors indicating positive connectivity and cool colors indicating negative connectivity. T-maps are thresholded at $p < 0.001$ and only clusters at $p < 0.05$ FWE corrected are shown. (B) Locations of the target ROIs (Table 4) chosen as peaks in the positive and negative average network. Numbered regions in orange indicate target ROIs from the positive network and regions indicated by letters in blue are negative target ROIs. 1 = ventrolateral prefrontal cortex (VLPFC), 2 = dorsolateral prefrontal cortex (DLPFC), 3 = putative human frontal eye fields (hFEF), 4 = sensorimotor (SM), 5 = fusiform gyrus (FG), 6 = peri-calcarine cortex (Calc), 7 = occipito-temporal (OT), 8 = mid occipital (MO), 9 = posterior thalamus (PT), A = ventromedial prefrontal cortex (VMPFC), B = inferior parietal lobule (IPL), C = precuneus (PCUN), D = middle temporal (Mid Temp), E = caudate nucleus (CN).

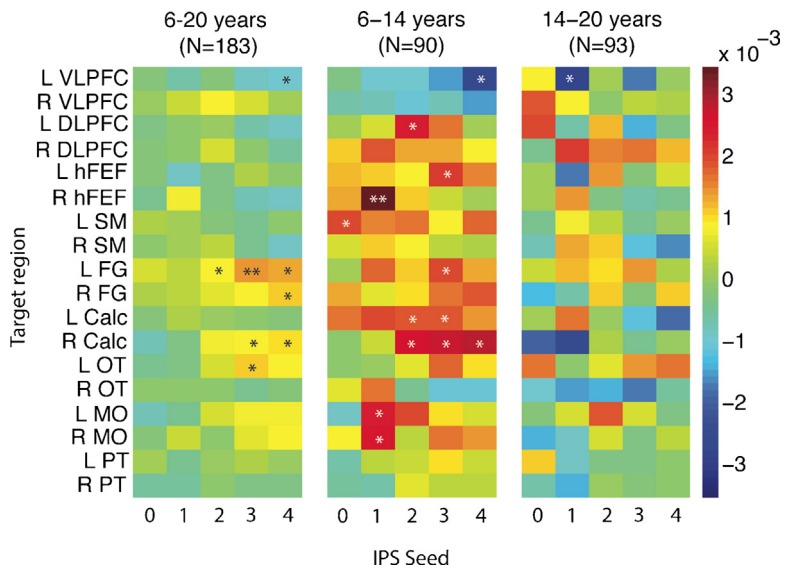


Fig. 5. Parameter estimates (β) for effects of age on functional connectivity to positive targets. Models were run separately for the whole sample (left panel), younger (middle panel) and older (right panel) sub-groups. VLPFC = ventrolateral prefrontal cortex, DLPFC = dorsolateral prefrontal cortex, hFEF = putative human frontal eye fields, SM = sensorimotor, FG = fusiform gyrus, Calc = peri-calcarine cortex, OT = occipito-temporal, MO = middle occipital, PT = posterior thalamus, L = left, R = right. * $p < 0.05$, ** $p < 0.005$.

Table 4

Location of the positive and negative target ROIs. These target ROIs were derived from peaks in the average network map shown in Fig. 4A. The ROI numbers and letters in column two refer to the regions indicated in Fig. 4B.

ROI	ID	Left ROI MNI coordinates			Right ROI MNI coordinates			
		x	y	z	x	y	z	
Positive target ROIs								
<i>Prefrontal</i>								
VLPFC	1	-50	30	24	52	38	14	
DLPFC	2	-48	2	34	48	6	30	
hFEF	3	-26	-4	52	28	-2	52	
SM	4	-49	-24	45	49	-24	45	
<i>Visual</i>								
FG	5	-30	-52	-14	30	-46	-14	
Calc	6	-22	-62	14	22	-62	14	
OT	7	-46	-66	-8	50	-62	-10	
MO	8	-36	-82	18	36	82	18	
<i>Subcortical</i>								
PT	9	-18	-32	0	20	-30	2	
Negative target ROIs								
<i>Frontal</i>								
VMPFC	A	-4	48	10	4	48	10	
<i>Parietal</i>								
IPL	B	-56	-60	32	58	-54	34	
PCUN	C	-6	-52	30	6	-52	30	
<i>Temporal</i>								
Mid temp	D	-60	-24	-12	60	-22	-8	
<i>Subcortical</i>								
CN	E	-16	18	14	14	16	18	

VLPFC = ventrolateral prefrontal cortex; DLPFC = dorsolateral prefrontal cortex; hFEF = putative human frontal eye fields; SM = sensorimotor; FG = fusiform gyrus; Calc = pericalcarine cortex; OT = occipito-temporal; MO = mid occipital; PT = posterior thalamus; VMPFC = ventromedial prefrontal cortex; IPL = inferior parietal lobule; PCUN = precuneus; Mid Temp = middle temporal; CN = caudate nucleus.

whole-brain corrected level, age-related variability was relatively subtle, and most prominent with ventral visual/fusiform regions.

Follow-up ROI analyses showed that within the network that is positively connected with the IPS, parameter estimates were generally more positive in the younger (6–14 years) than the older group (14–20 years), across both prefrontal and visual targets. In contrast, for the targets that show on average negative connectivity with the IPS, age-effects were generally more negative in the older group. This suggests that perhaps changes in pre-adolescent connectivity appear largely as within-network enhancement, while across adolescence task-positive and negative networks become more antagonistic, a hypothesis that could ideally be tested in an independent longitudinal sample.

The main hypothesis of the present investigation, that there is a positive association between IPS-to-prefrontal functional

connectivity with age was largely not borne out, though positive trends were identified in ROI analyses in the younger age group. Results from previous intrinsic functional connectivity studies have been mixed (Barber et al., 2013; Jolles et al., 2011; Uddin et al., 2011). Evidence supporting the hypothesis for increased fronto-parietal connectivity with age comes from both the observation that functional activation patterns in frontal and parietal cortices increase with age and working memory capacity (Crone et al., 2006; Klingberg et al., 2002; Scherf et al., 2006), and robust evidence for changes in properties of fronto-parietal white matter structure (Lebel and Beaulieu, 2011). The present study aimed to overcome possible limitations of previous work, using a relatively large sample size, and hypothesis driven analyses that allowed for differences in functional connectivity patterns at different sites along the IPS. A limitation of our study is the heterogeneity in acquisition

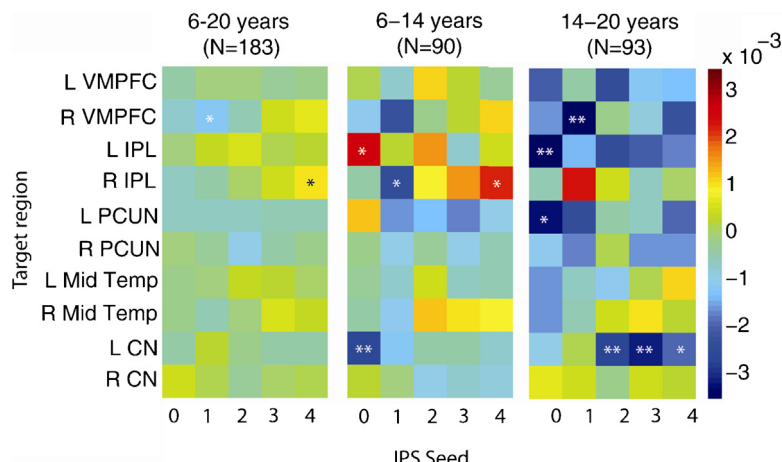


Fig. 6. Parameter estimates (β) for effects of age on functional connectivity to negative targets. Models were run separately for the whole sample (left panel), younger (middle panel) and older (right panel) sub-groups. VMPFC = ventromedial prefrontal, IPL = inferior parietal lobule, PCUN = precuneus, Mid Temp = middle temporal, CN = caudate nucleus, L = left, R = right. * $p < 0.05$, ** $p < 0.005$.

parameters across data collection sites, which may have affected our ability to resolve age-effects.

We hypothesized that we would find a positive association with age between anterior IPS seeds and prefrontal regions such as the DLPFC (Barber et al., 2013). At the whole-brain level, we instead found positive age-associations between anterior IPS seeds bilaterally and ventral visual fusiform regions. This was consistent with ROI analyses, which showed that across the sample significantly positive age-effects were largely limited to anterior IPS to visual region connectivity, including fusiform, pericalcarine and occipito-temporal regions. We note that though ventral visual regions showed on average greater functional connectivity to posterior IPS0 and 1, these were also significant in IPS3 and 4 models. Although the dorsal and ventral visual streams are presumed to support distinct object- and spatial-visual processing (Goodale and Milner, 1992), they nonetheless must interact for the production of complex behaviors (Cloutman, 2013). The finding that connectivity between anterior IPS and ventral visual regions increases over the course of adolescence may reflect a maturation of complex cognitive processes relying on dorsal-to-ventral stream interactions. However, as this finding was unexpected given our *a priori* hypotheses, it should be independently replicated.

At the whole-brain level, a negative age-association was found for right IPS1 in relation to medial orbitofrontal cortex. This region was on average anti-correlated with the IPS1 seed and is often included in descriptions of the default mode network (Fox et al., 2005). Although this was a fairly restricted effect, it is consistent with recent work showing that with increasing age, functional networks such as the DAN and DMN become more distinct (Barber et al., 2013; Chai et al., 2014). At the ROI level, however, we did not find broad age-increases in anti-correlation between the IPS and targets in DMN-associated regions, although negative age trends were apparent in the older sub-sample. Also at the whole-brain level, IPS2, 3 and 4 each showed negative age-effects in anterior superior parietal/superior post-central gyrus regions. This negative age-effect occurred within regions that are nonetheless positively connected with the seed regions. This pattern suggests that local functional connectivity may be more specific/refined with age in the superior parietal cortex.

Additional positive associations with age were found, at the whole-brain level, between left IPS0 and right superior temporal cortex, and at the ROI level between right IPS4 and inferior parietal lobule. These findings were unexpected and challenging to interpret, but suggest that age-effects on functional connectivity patterns may be challenging to simplify in terms of within-network increases and between network-decreases with age.

Increasing fronto-parietal functional connectivity with age, and changes in white matter structure, have been suggested as a mechanism underlying developmental increases in attentional and working memory capacity (Edin et al., 2007; Klarborg et al., 2013; Klingberg et al., 2002; Mabbott et al., 2006). Indeed, increased BOLD activity in frontal and parietal regions with increased working memory capacity has been shown in several developmental neuroimaging studies (Crone et al., 2006; Klingberg et al., 2002; Scherf et al., 2006). Among seed regions tested here, age-related variability in fronto-parietal resting connectivity was relatively more positive in right IPS1 to hFEF, compared to other IPS seeds. Although previous studies have shown increases in resting connectivity between IPS and DLPFC with age (Barber et al., 2013), we did not observe an age-related increase in IPS to VLPFC or DLPFC connectivity across this sample, though ROI analyses showed a positive trend with age between left DLPFC and IPS2 in the younger sub-sample. Generally speaking, a longitudinal or working memory task design may be more sensitive to these effects. It is also notable that while some studies support increased long-range connectivity with development and weakening short-range connections (Dosenbach et al.,

2010; Fair et al., 2008), studies using more stringent controls for head motion have had more variable findings (Chai et al., 2014).

Aberrant functional connectivity of the IPS and adjacent superior and inferior parietal lobules has been reported in several disorders affecting attention, including Autism Spectrum Disorders (ASD) (Nielsen et al., 2013), Turner syndrome (Bray et al., 2011, 2013c), 22q11.2 deletion syndrome (Simon et al., 2008), children born preterm (Doesburg et al., 2013; Scheinost et al., 2014), and Attention Deficit Hyperactivity Disorder (Tomasi and Volkow, 2012). Structural and functional connectivity patterns of the IPS suggest that this is a key node in the network of regions important for visual attention. Disruption of any one of many connections could have an impact on functioning of the IPS, resulting in a similar cognitive phenotype, marked by impaired attention. Future work in this area should consider the specific location within the IPS when assessing connectivity differences, as a body of work now points to differential functional roles and connectivity patterns of regions along the IPS (Anderson et al., 2010; Greenberg et al., 2012; Mars et al., 2011). Ultimately, approaches to intervention may vary depending on specific patterns of affected structural or functional connectivity.

A strength of this study is the use of a set of IPS seed regions known to have differing structural connectivity patterns. Resting-state functional connectivity analyses, including developmental studies, have typically used either a data-driven approach, such as ICA (e.g. Uddin et al., 2011) or a seed-based approach (e.g. Fair et al., 2008). Here, we have used relatively small seeds defined from previous functional studies. We note that despite proximity of these seeds to one another, region-specific patterns of both connectivity and age-related variability can be observed. These patterns would be obscured using larger seed-regions, highlighting the importance of choosing both the size and location of seed regions for connectivity analyses based on addressing specific hypotheses.

There are several limitations associated with this study. The inherent limitations of resting functional connectivity have been well described elsewhere (Buckner et al., 2013), and include: an imperfect relationship to anatomical connections, dependence on mental state which may differ across individuals 'at rest' and lack of baseline or control condition. More specific to this study, coordinates corresponding to IPS regions 0–4 were selected from a previous study, rather than within subject localization, potentially contributing to heterogeneity across subjects. A related concern is that it is not known how the size and location of these regions might vary with age, and coordinates used here were from a study performed in young adults. Data in this study were pooled from several sites that used different fMRI protocols. The effect of site was modeled in all group-level analyses, but may nonetheless have contributed additional variability that could reduce significance of reported effects. For example, scan duration in this same sample influenced the ability to classify subjects as ASD or TD based on connectivity patterns (Nielsen et al., 2013). We performed secondary analyses on data with similar run lengths across sites, and found largely similar effects. The sample in this study was more heavily biased toward males, because the data were initially collected as control samples for ASD studies. Finally, with the present approach we cannot rule out vascular effects on age-related variability in connectivity (Scheinost et al., 2014).

5. Conclusions

In conclusion, we present here an investigation into region-specific age-related variability in functional connectivity along the posterior-to-anterior axis of the IPS. The strongest positive age-effects were observed between ventral visual and peri-calcarine cortex and anterior IPS 3 and 4. Negative age-effects were most

prominent in anterior superior parietal cortex. Our results suggest that IPS functional connectivity is largely established by age 6, but that this network nonetheless undergoes connectivity maturation, which may play an important role in cognitive maturation across this period. The findings presented here lay a critical foundation for studying divergent patterns of connectivity, and effects of age, in populations with structural or functional abnormalities in the IPS (Bray et al., 2011; Keehn et al., 2013; Tomasi and Volkow, 2012).

Conflict of interest statement

None declared.

Funding

Sources of funding for the New York University Langone Medical Centre include: NIH (K23MH087770; R21MH084126; R01MH081218; R01HD065282), Autism Speaks, The Stavros Niarchos Foundation, The Leon Levy Foundation, and an endowment from Phyllis Green and Randolph Cowan. Funding for the University of Michigan samples one and two includes: NIH (U19 HD0354821; MH066496 (CL); R21 MH079871 (SP)), Autism Speaks (CSM), an Autism Speaks Pre-doctoral Fellowship 4773 (JLW), and a Michigan Institute for Clinical and Health Research Pre-Doctoral Fellowship UL1RR024986 (JLW). Funding for the University of Utah School of Medicine includes: NIH (K08 MH092697; R01MH080826; P50MH60450; T32DC008553; R01NS34783), the Ben B. and Iris M. Margolis Foundation, an Autism Speaks Mentor-Based Predoctoral Fellowship (1677), a University of Utah Multidisciplinary Research Seed Grant, and a NRSA Predoctoral Fellowship (F31 DC010143). Funding for the Yale Child Study Centre includes: Simons Foundation (KP), Autism Speaks (KP), John Merck Scholars Fund (KP), Autism Science Foundation, NICHD (KP), and NIMH.

Acknowledgements

The authors want to acknowledge the sources of funding that made this analysis possible including an NSERC Discovery Grant (SB) and a SickKids Foundation New Investigator Grant (SB) as well as the Alberta Children's Hospital Foundation (SB). These funders (SB) played no role in the design, execution or publication of this study.

Appendix A. Supplementary data

Supplementary data associated with this article can be found, in the online version, at <http://dx.doi.org/10.1016/j.dcn.2015.04.004>

References

- Anderson, J.C., Kennedy, H., Martin, K.A., 2011. Pathways of attention: synaptic relationships of frontal eye field to V4, lateral intraparietal cortex, and area 46 in macaque monkey. *J. Neurosci.* 31, 10872–10881.
- Anderson, J.S., Ferguson, M.A., Lopez-Larson, M., Yurgelun-Todd, D., 2010. Topographic maps of multisensory attention. *Proc. Natl. Acad. Sci. U. S. A.* 107, 20110–20114.
- Astafiev, S.V., Shulman, G.L., Stanley, C.M., Snyder, A.Z., Van Essen, D.C., Corbetta, M., 2003. Functional organization of human intraparietal and frontal cortex for attending, looking, and pointing. *J. Neurosci.* 23, 4689–4699.
- Auzias, G., Viellard, M., Takerkart, S., Villeneuve, N., Poinsot, F., Fonséca, D.D., Girard, N., et al., 2014. Atypical sulcal anatomy in young children with autism spectrum disorder. *Neuroimage Clin.* 4, 593–603.
- Barber, A.D., Caffo, B.S., Pekar, J.J., Mostofsky, S.H., 2013. Developmental changes in within- and between-network connectivity between late childhood and adulthood. *Neuropsychologia* 51, 156–167.
- Blakemore, S.J., 2012. Imaging brain development: the adolescent brain. *Neuroimage* 61, 397–406.
- Bray, S., Almas, R., Arnold, A.E., Iaria, G., Macqueen, G., 2013a. Intraparietal sulcus activity and functional connectivity supporting spatial working memory manipulation. *Cereb. Cortex* (Epub ahead of print).
- Bray, S., Arnold, A.E., Iaria, G., Macqueen, G., 2013b. Structural connectivity of visuotopic intraparietal sulcus. *Neuroimage* 82, 137–145.
- Bray, S., Dunkin, B., Hong, D.S., Reiss, A.L., 2011. Reduced functional connectivity during working memory in Turner syndrome. *Cereb. Cortex* 21, 2471–2481.
- Bray, S., Hoeft, F., Hong, D.S., Reiss, A.L., 2013c. Aberrant functional network recruitment of posterior parietal cortex in Turner syndrome. *Hum. Brain Mapp.* 34, 3117–3128.
- Brett, M., Anton, J., Valabregue, R., Poline, J., 2002. Region of interest analysis using an SPM toolbox [abstract]. In: The 8th International Conference on Functional Mapping of the Human Brain.
- Buckner, R.L., Krienen, F.M., Yeo, B.T., 2013. Opportunities and limitations of intrinsic functional connectivity MRI. *Nat. Neurosci.* 16, 832–837.
- Cantlon, J.F., Li, R., 2013. Neural activity during natural viewing of Sesame Street statistically predicts test scores in early childhood. *PLoS Biol.* 11, e1001462.
- Chai, X.J., Ofen, N., Gabrieli, J.D., Whitfield-Gabrieli, S., 2014. Selective development of anticorrelated networks in the intrinsic functional organization of the human brain. *J. Cogn. Neurosci.* 26, 501–513.
- Champod, A.S., Petrides, M., 2007. Dissociable roles of the posterior parietal and the prefrontal cortex in manipulation and monitoring processes. *Proc. Natl. Acad. Sci. U. S. A.* 104, 14837–14842.
- Cloutman, L.L., 2013. Interaction between dorsal and ventral processing streams: where, when and how? *Brain Lang.* 127, 251–263.
- Corbetta, M., Kincade, J.M., Ollinger, J.M., McAvoi, M.P., Shulman, G.L., 2000. Voluntary orienting is dissociated from target detection in human posterior parietal cortex. *Nat. Neurosci.* 3, 292–297.
- Crone, E.A., Wendelken, C., Donohue, S., van Leijenhorst, L., Bunge, S.A., 2006. Neurocognitive development of the ability to manipulate information in working memory. *Proc. Natl. Acad. Sci. U. S. A.* 103, 9315–9320.
- de Bie, H.M., Boersma, M., Adriaanse, S., Veltman, D.J., Wink, A.M., Roosendaal, S.D., Barkhof, F., et al., 2012. Resting-state networks in awake five- to eight-year old children. *Hum. Brain Mapp.* 33, 1189–1201.
- de Bie, H.M., Boersma, M., Wattjes, M.P., Adriaanse, S., Vermeulen, R.J., Oostrom, K.J., Huisman, J., et al., 2010. Preparing children with a mock scanner training protocol results in high quality structural and functional MRI scans. *Eur. J. Pediatr.* 169, 1079–1085.
- Dehaene, S., Piazza, M., Pinel, P., Cohen, L., 2003. Three parietal circuits for number processing. *Cogn. Neuropsychol.* 20, 487–506.
- Di Martino, A., Yan, C.G., Li, Q., Denio, E., Castellanos, F.X., Alaerts, K., Anderson, J.S., et al., 2014. The autism brain imaging data exchange: towards a large-scale evaluation of the intrinsic brain architecture in autism. *Mol. Psychiatry* 19, 659–667.
- Doesburg, S.M., Moiseev, A., Herdman, A.T., Ribary, U., Grunau, R.E., 2013. Region-specific slowing of alpha oscillations is associated with visual-perceptual abilities in children born very preterm. *Front. Hum. Neurosci.* 7, 791.
- Dosenbach, N.U., Nardos, B., Cohen, A.L., Fair, D.A., Power, J.D., Church, J.A., Nelson, S.M., et al., 2010. Prediction of individual brain maturity using fMRI. *Science* 329, 1358–1361.
- Edin, F., Macoveanu, J., Olesen, P., Tegnér, J., Klingberg, T., 2007. Stronger synaptic connectivity as a mechanism behind development of working memory-related brain activity during childhood. *J. Cogn. Neurosci.* 19, 750–760.
- Fair, D.A., Cohen, A.L., Dosenbach, N.U., Church, J.A., Miezin, F.M., Barch, D.M., Raichle, M.E., et al., 2008. The maturing architecture of the brain's default network. *Proc. Natl. Acad. Sci. U. S. A.* 105, 4028–4032.
- Fair, D.A., Dosenbach, N.U., Church, J.A., Cohen, A.L., Brahmbhatt, S., Miezin, F.M., Barch, D.M., et al., 2007. Development of distinct control networks through segregation and integration. *Proc. Natl. Acad. Sci. U. S. A.* 104, 13507–13512.
- Farrant, K., Uddin, L.Q., 2015. Asymmetric development of dorsal and ventral attention networks in the human brain. *Dev. Cogn. Neurosci.* 12, 165–174.
- Fox, M.D., Snyder, A.Z., Vincent, J.L., Corbetta, M., Van Essen, D.C., Raichle, M.E., 2005. The human brain is intrinsically organized into dynamic, anticorrelated functional networks. *Proc. Natl. Acad. Sci. U. S. A.* 102, 9673–9678.
- Friston, K., 1994. Functional and effective connectivity in neuroimaging: a synthesis. *Hum. Brain Mapp.* 2, 56–78.
- Gogtay, N., Giedd, J.N., Lusk, L., Hayashi, K.M., Greenstein, D., Vaituzis, A.C., Nugent, T.F., et al., 2004. Dynamic mapping of human cortical development during childhood through early adulthood. *Proc. Natl. Acad. Sci. U. S. A.* 101, 8174–8179.
- Goodale, M.A., Milner, A.D., 1992. Separate visual pathways for perception and action. *Trends Neurosci.* 15, 20–25.
- Greenberg, A.S., Verstynen, T., Chiu, Y.C., Yantis, S., Schneider, W., Behrmann, M., 2012. Visuotopic cortical connectivity underlying attention revealed with white-matter tractography. *J. Neurosci.* 32, 2773–2782.
- Greicius, M.D., Supekar, K., Menon, V., Dougherty, R.F., 2009. Resting-state functional connectivity reflects structural connectivity in the default mode network. *Cereb. Cortex* 19, 72–78.
- Hutchinson, J.B., Uncapher, M.R., Wagner, A.D., 2015. Increased functional connectivity between dorsal posterior parietal and ventral occipitotemporal cortex during uncertain memory decisions. *Neurobiol. Learn. Mem.* 117, 71–83.
- Jolles, D.D., van Buchem, M.A., Crone, E.A., Rombouts, S.A., 2011. A comprehensive study of whole-brain functional connectivity in children and young adults. *Cereb. Cortex* 21, 385–391.
- Kahnt, T., Chang, L.J., Park, S.Q., Heinze, J., Haynes, J.D., 2012. Connectivity-based parcellation of the human orbitofrontal cortex. *J. Neurosci.* 32, 6240–6250.
- Keehn, B., Müller, R.A., Townsend, J., 2013. Atypical attentional networks and the emergence of autism. *Neurosci. Biobehav. Rev.* 37, 164–183.

- Kesler, S.R., Haberrecht, M.F., Menon, V., Warsovsky, I.S., Dyer-Friedman, J., Neely, E.K., Reiss, A.L., 2004. Functional neuroanatomy of spatial orientation processing in Turner syndrome. *Cereb. Cortex* **14**, 174–180.
- Kesler, S.R., Menon, V., Reiss, A.L., 2006. Neuro-functional differences associated with arithmetic processing in Turner syndrome. *Cereb. Cortex* **16**, 849–856.
- Klarborg, B., Skak Madsen, K., Vestergaard, M., Skimminge, A., Jernigan, T.L., Baaré, W.F., 2013. Sustained attention is associated with right superior longitudinal fasciculus and superior parietal white matter microstructure in children. *Hum. Brain Mapp.* **34**, 3216–3232.
- Klingberg, T., Forssberg, H., Westerberg, H., 2002. Increased brain activity in frontal and parietal cortex underlies the development of visuospatial working memory capacity during childhood. *J. Cogn. Neurosci.* **14**, 1–10.
- Lebel, C., Walker, L., Leemans, A., Phillips, L., Beaulieu, C., 2008. Microstructural maturation of the human brain from childhood to adulthood. *Neuroimage* **40**, 1044–1055.
- Lebel, C., Beaulieu, C., 2011. Longitudinal development of human brain wiring continues from childhood into adulthood. *J. Neurosci.* **31**, 10937–10947.
- Liu, H., Qin, W., Li, W., Fan, L., Wang, J., Jiang, T., Yu, C., 2013. Connectivity-based parcellation of the human frontal pole with diffusion tensor imaging. *J. Neurosci.* **33**, 6782–6790.
- Mabbott, D.J., Noseworthy, M., Bouffet, E., Laughlin, S., Rockel, C., 2006. White matter growth as a mechanism of cognitive development in children. *Neuroimage* **33**, 936–946.
- Mars, R.B., Jbabdi, S., Sallet, J., O'Reilly, J.X., Croxson, P.L., Olivier, E., Noonan, M.P., et al., 2011. Diffusion-weighted imaging tractography-based parcellation of the human parietal cortex and comparison with human and macaque resting-state functional connectivity. *J. Neurosci.* **31**, 4087–4100.
- Mazaika, P., Hoeft, F., Glover, G., Reiss, A., 2009. Methods and software for fMRI analysis for clinical subjects. Poster presented at the 15th Annual Meeting for the Organization of Human Brain Mapping.
- Moayedi, M., Salomons, T.V., Dunlop, K.A., Downar, J., Davis, K.D., 2014. Connectivity-based parcellation of the human frontal polar cortex. *Brain Struct. Funct.* (Epub ahead of print).
- Molko, N., Cachia, A., Riviere, D., Mangin, J.F., Bruandet, M., Le Bihan, D., Cohen, L., et al., 2003. Functional and structural alterations of the intraparietal sulcus in a developmental dyscalculia of genetic origin. *Neuron* **40**, 847–858.
- Nagy, Z., Westerberg, H., Klingberg, T., 2004. Maturation of white matter is associated with the development of cognitive functions during childhood. *J. Cogn. Neurosci.* **16**, 1227–1233.
- Nelson, S.M., Cohen, A.L., Power, J.D., Wig, G.S., Miezin, F.M., Wheeler, M.E., Velanova, K., et al., 2010. A parcellation scheme for human left lateral parietal cortex. *Neuron* **67**, 156–170.
- Nielsen, J.A., Zielinski, B.A., Fletcher, P.T., Alexander, A.L., Lange, N., Bigler, E.D., Lainhart, J.E., et al., 2013. Multisite functional connectivity MRI classification of autism: ABIDE results. *Front. Hum. Neurosci.* **7**, 599.
- Nordahl, C.W., Dierker, D., Mostafavi, I., Schumann, C.M., Rivera, S.M., Amaral, D.G., Van Essen, D.C., 2007. Cortical folding abnormalities in autism revealed by surface-based morphometry. *J. Neurosci.* **27**, 11725–11735.
- Østby, Y., Tamnes, C.K., Fjell, A.M., Walhovd, K.B., 2011. Morphometry and connectivity of the fronto-parietal verbal working memory network in development. *Neuropsychologia* **49**, 3854–3862.
- Pessoa, L., Gutierrez, E., Bandettini, P., Ungerleider, L., 2002. Neural correlates of visual working memory: fMRI amplitude predicts task performance. *Neuron* **35**, 975–987.
- Pinel, P., Dehaene, S., Rivière, D., LeBihan, D., 2001. Modulation of parietal activation by semantic distance in a number comparison task. *Neuroimage* **14**, 1013–1026.
- Power, J.D., Barnes, K.A., Snyder, A.Z., Schlaggar, B.L., Petersen, S.E., 2012. Spurious but systematic correlations in functional connectivity MRI networks arise from subject motion. *Neuroimage* **59**, 2142–2154.
- Power, J.D., Cohen, A.L., Nelson, S.M., Wig, G.S., Barnes, K.A., Church, J.A., Vogel, A.C., et al., 2011. Functional network organization of the human brain. *Neuron* **72**, 665–678.
- Rosenberg-Lee, M., Barth, M., Menon, V., 2011. What difference does a year of schooling make? Maturation of brain response and connectivity between 2nd and 3rd grades during arithmetic problem solving. *Neuroimage* **57**, 796–808.
- Rubia, K., 2013. Functional brain imaging across development. *Eur. Child Adolesc. Psychiatry* **22**, 719–731.
- Scheinost, D., Lacadie, C., Vohr, B.R., Schneider, K.C., Papademetris, X., Constable, R.T., Ment, L.R., 2014. Cerebral lateralization is protective in the very prematurely born. *Cereb. Cortex* (Epub ahead of print).
- Scherf, K.S., Sweeney, J.A., Luna, B., 2006. Brain basis of developmental change in visuospatial working memory. *J. Cogn. Neurosci.* **18**, 1045–1058.
- Sereno, M.I., Pitzalis, S., Martinez, A., 2001. Mapping of contralateral space in retinotopic coordinates by a parietal cortical area in humans. *Science* **294**, 1350–1354.
- Shaw, P., Kabani, N.J., Lerch, J.P., Eckstrand, K., Lenroot, R., Gogtay, N., Greenstein, D., et al., 2008. Neurodevelopmental trajectories of the human cerebral cortex. *J. Neurosci.* **28**, 3586–3594.
- Sheremata, S.L., Bettencourt, K.C., Somers, D.C., 2010. Hemispheric asymmetry in visuotopic posterior parietal cortex emerges with visual short-term memory load. *J. Neurosci.* **30**, 12581–12588.
- Silver, M.A., Kastner, S., 2009. Topographic maps in human frontal and parietal cortex. *Trends Cogn. Sci. (Regul. Ed.)* **13**, 488–495.
- Simon, T.J., Wu, Z., Avants, B., Zhang, H., Gee, J.C., Stebbins, G.T., 2008. Atypical cortical connectivity and visuospatial cognitive impairments are related in children with chromosome 22q11.2 deletion syndrome. *Behav. Brain Funct.* **4**, 25.
- Supekar, K., Musen, M., Menon, V., 2009. Development of large-scale functional brain networks in children. *PLoS Biol.* **7**, e1000157.
- Swisher, J.D., Halko, M.A., Merabet, L.B., McMains, S.A., Somers, D.C., 2007. Visual topography of human intraparietal sulcus. *J. Neurosci.* **27**, 5326–5337.
- Szczepanski, S.M., Pinsky, M.A., Douglas, M.M., Kastner, S., Saalmann, Y.B., 2013. Functional and structural architecture of the human dorsal frontoparietal attention network. *Proc. Natl. Acad. Sci. U. S. A.* **110**, 15806–15811.
- Tomasi, D., Volkow, N.D., 2012. Abnormal functional connectivity in children with attention-deficit/hyperactivity disorder. *Biol. Psychiatry* **71**, 443–450.
- Toro, R., Fox, P.T., Paus, T., 2008. Functional coactivation map of the human brain. *Cereb. Cortex* **18**, 2553–2559.
- Uddin, L.Q., Supekar, K.S., Ryali, S., Menon, V., 2011. Dynamic reconfiguration of structural and functional connectivity across core neurocognitive brain networks with development. *J. Neurosci.* **31**, 18578–18589.
- Vandenbergh, R., Molenberghs, P., Gillebert, C.R., 2012. Spatial attention deficits in humans: the critical role of superior compared to inferior parietal lesions. *Neuropsychologia* **50**, 1092–1103.
- Westerberg, H., Hirvikoski, T., Forssberg, H., Klingberg, T., 2004. Visuo-spatial working memory span: a sensitive measure of cognitive deficits in children with ADHD. *Child Neuropsychol.* **10**, 155–161.
- Zhan, J.Y., Wilding, J., Cornish, K., Shao, J., Xie, C.H., Wang, Y.X., Lee, K., et al., 2011. Charting the developmental trajectories of attention and executive function in Chinese school-aged children. *Child Neuropsychol.* **17**, 82–95.